Sławomir OWCZARZAK*, Andrzej STAFINIAK, Joanna PRAŻMOWSKA, Regina PASZKIEWICZ

Faculty of Microsystem Electronics and Phtonics, Wrocław University of Science and Technology, Wrocław, Poland

Study of the side walls inclination angle after RIE process of piezotronic structures

Abstract. Control of geometric features of fabricated semiconductors structures such as shape, depth and slope of side walls allows precize control the shape of fabricated piezotronic devices. The electrical response of the piezotronic materials is the most significant when the frequency of the input mechanical signal corresponds to the resonant frequency of the structure. The resonant frequency of the structures is defined by the structures properties and geometry. Therefore, the main aim of piezotronic structures fabrication during reactive ion etching process is receiving the assumed geometrical features. The fabrication of GaN structures with assumed geometric features requires taking into account parameters such as: inclination side walls angle of mask, selectivity of etching [semiconductor: mask], density and width of pattern, and target depth of structures. In this article, the half-empirical equation and the results of research on GaN structures inclination side walls angle evolution in function of pattern width were presented.

Streszczenie. Kontrola geometrycznych parametrów wytwarzanych półprzewodnikowych struktur, takich jak: kształt, głębokość i kąt nachylenia ścian bocznych, umożliwia precyzyjną kontrolę kształtu wytwarzanych przyrządów piezotronicznych. Odpowiedź elektryczna materiałów piezotronicznych jest największa, gdy częstotliwość sygnału mechanicznego odpowiada częstotliwości rezonansowej struktury. Częstotliwość rezonansowa struktury zależy od właściwości materiałowych oraz kształtu. Z tego powodu, głównym celem kształtowania struktur piezotronicznych w procesie reaktywnego trawienia jonowego jest otrzymywanie struktur o zadanych wymiarach geometrycznych. Otrzymywanie struktur GaN o zadanej geometrii wymaga uwzględnienia parametrów procesu trawienia, takich jak: kąta nachylenia ścian bocznych maski, selektywność trawienia, gęstość trawionych wzorów, szerokość wzoru oraz docelowa głębokość struktury. W artykule przedstawiono pół-empiryczne równanie i wyniki badań dotyczących wpływu szerokości wzoru na kąt nachylenia ścian bocznych struktur GaN. Badanie kąta nachylenia ścian bocznych struktur piezotronicznych po procesie RIE

Słowa kluczowe: GaN, trencze, ISWA
Keywords: GaN, trenches, ISWA

Introduction

Besides of the parameters of RIE process, in order to obtain the intended geometric shape of structures after reactive ion etching (RIE) such as depth and inclination side walls angle (ISWA) should be include the shape of mask, and pattern size and density. The Macro-loading effect or Loading effect is drop of etch rate in function of increased: numbers of samples or global area of etched surface. The Micro-loading effect is drop of etch rate in function of increased local area of etched surface, and increased pattern density, on one sample. The Profile-loading effect is defined as difference of side walls slope between trenches in cascade order, and external or insulated trenches. The ARDE (aspect ratio dependent etch) phenomenon is drop of etch rate in function of increased depth to width ratio, or in function of RIE process duration [1]. Indeed the macro-loading and the micro-loading effects are result of depleted reagent concentration caused by increased area to be etched trough more density or width of pattern or total etched surface area. Increased concentration of etching products changes the impedance of plasma sheath over the etched surface, and it leads to decrease of etch rate [2, 3]. The micro-loading effect is possible to limited using very low pressure in chamber, such as in electron cyclotron resonance (ECR) etching system [4]. The ARDE effect is caused by decreasing ion current in function of structures depth as result of more complicated ion Ar$^+$ migration to the surface, and deteriorated ability to remove etching products from the surface [5, 6]. Several mathematical description of ARDE effect was made in the literature [7, 8, 9]. The RIE-lag effect is drop of etch rate in function of less width pattern. It is result of asymmetrical electric dipole focused around the trenches caused by accumulation of positive charges on the mask surface and negative charges inside the structure [6]. The electrical diffusing lens for positive argon ions are formed by accumulated positive charges on the mask edges. The electric field is the strongest near the edges of the structures, thus the deviation of the ion trajectory is the most significant during etching of the narrowest trenches. The accumulated, positive charges on the trenches edge, which create the diffuse lens for positive ions, cause decreasing etch rate of patterns with smaller widths. However, accumulation of negative charges on the trenches edge create focusing lens for positive ions and cause increased etch rate of patterns with smaller widths. This effect is named anty-RIE lag [6]. The piezoelectricity phenomenon is observed in semiconductors materials III-V and II-VI, which have non-central symmetry crystals with hexagonal wurtzite or cubic zinc blende structures such as: ZnO, GaAs, InAs, InGaAs, GaN, AlN, InN, AlGaN, and InGaN. Therefore, the ISWA of GaN structures after RIE process for the piezotronic and vertical semiconductors devices are deeply studied. In the literature noticed dependence of structures ISWA after RIE process from mask ISWA and pattern width, however, not shown any mathematical description [10]. In this article the proposal of mathematical description of influence of mask ISWA and pattern width on structures ISWA, obtained after RIE process is presented.

Experiment details

On the sapphire substrates were grown approximately 2 μm epitaxial GaN layers using metal organic vapour phase epitaxy (MOVPE). On the GaN/sapphire, different thickness of silicon dioxide layers were deposited using plasma enhanced chemical vapour deposition (PECVD) technique. On the SiO$_2$/GaN/sapphire samples, the parallel stripes were patterned using photolithography, and developed using BHF solution for hard mask fabrication. In the Figure 1 the pattern of stripes fabricated in silicon dioxide layer is presented. All strips and trenches after RIE process were observed using scanning electron microscopy (SEM, Su6600 HITACHI). The electron beam in SEM was accelerated by 15 kV. In the Figure 2, the dependence of mask ISWA from silicon dioxide layer thickness a) and pattern width b) is presented. The measurements were obtained using Atomic Force Microscopy (AFM, Veeco MultiMode with NanoScope V Controller).
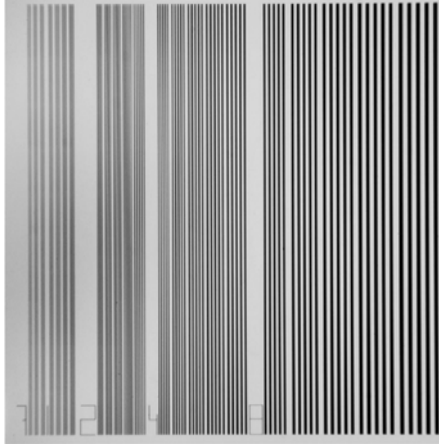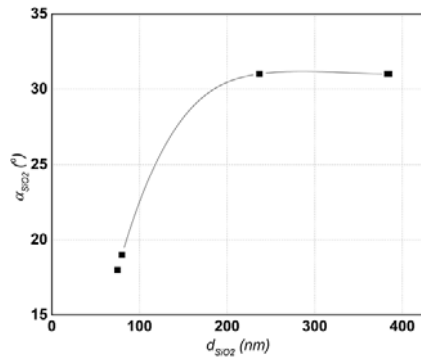
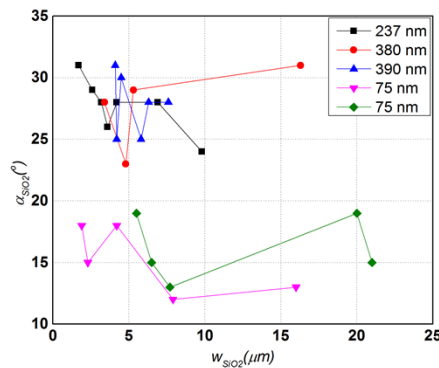Fig. 1 The stripes pattern studied during RIE process

a)

b)

Fig. 2 Dependence of hard-mask inclination from a) layer thickness and b) pattern width

The tip side walls of the AFM etched silicon probe is 17° from the vertical direction. Side walls inclination of mask increased with the thickness of the layer, reaching a maximum of 31° at thickness of 210 nm. Above the 200 nm thickness of silicon dioxide layer, no change of mask ISWA

was noted. The mask ISWA in function of pattern width was changed without a clear trend. The samples with stripes mask were processed using RIE in chamber with parallel, asymmetric electrodes using capacity coupled plasma. In the Table 1, used recipe of RIE process is presented. In this study is observed that the SiO$_2$ layer thickness has influence on ISWA of obtained hard-mask before RIE process, according to Eq. (1):

(1) $$\alpha_{SiO2} = A - B \cdot exp(- C \cdot d_{SiO2})$$

where α_{SiO2} is the SiO$_2$ mask ISWA, d_{SiO2} is the SiO$_2$ layer thickness, A = 31,12, B = 71, C = 0,02.

Table 1. Used recipe during capacity coupled plasma RIE process

Pressure [mTorr]	Temperature [°C]	RF power [W]	BCl$_3$/Cl$_2$/Ar [sccm]
15	7	250	16/4/5

Results and discussion

The structures side walls inclination obtained after RIE process depends on the etching selectivity [semiconductor: mask], and the mask side walls inclination. The Eqs (2 – 4) show theoretical influence of mask ISWA and etching selectivity on structures ISWA, only if ions are not scattered on the mask edge, and ions trajectory is perpendicular to the samples. Geometric interpretation of Eqs (2 – 4) is presented in Fig. 3.

(2) $$\frac{h}{b} = tg\Phi$$

(3) $$tg\alpha = \frac{s \cdot h}{b} = s \cdot tg\Phi$$

(4) $$\alpha = arctg(s \cdot tg\Phi)$$

where α is the structures angle, Φ is the mask angle, h is the etched mask thickness, b is the structures slope width, s is selectivity of etching [semiconductor: mask].

The SEM images of exemplary island and trench are presented respectively in Fig. 4: island (a) and trench (b). The width of structures was measured as the width between upper slopes edges of islands (w^j) and trenches (w^t) as well as the width between lower slopes edges of islands (w_i) and trenches (w_t). The AFM and SEM results of ISWA structures measurements were presented and compared in this study. The structures ISWA measured using AFM are presented in Fig. 5: in function of aspect ratio (AR) (a) and in function of trenches width (b). The all AFM results of ISWA presented in Fig. 5 (a) can not be described as the one equation with one variable such as aspect ratio. In the Fig. 5 (b) are presented ISWA results grouped by structures depth in function of structures width.
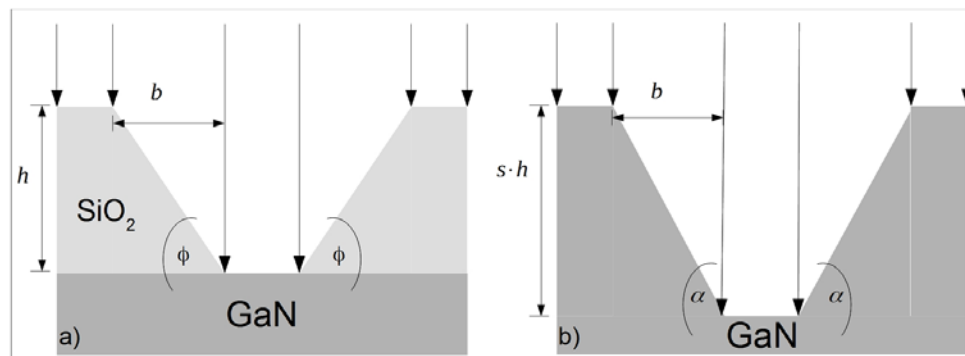

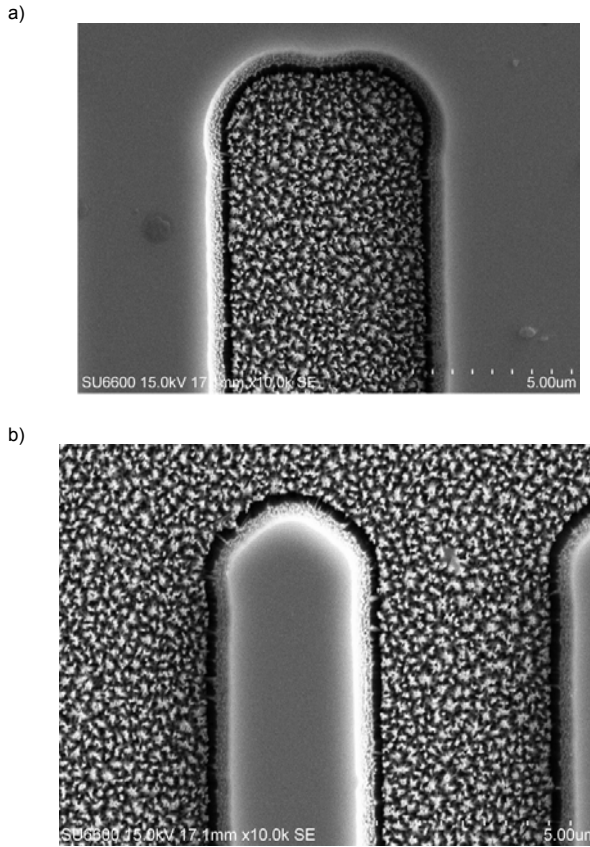Fig. 3 Influence of mask profile on obtained structure profile

a)

b)

Fig. 4 The SEM images of exemplary a) island and b) trench of 920 nm depth GaN structures after RIE process
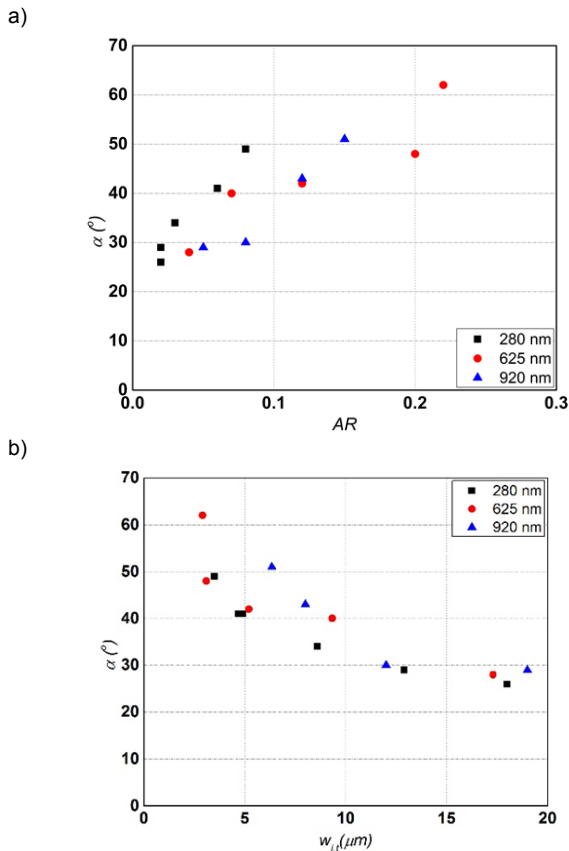
a)

b)

Fig. 5 The GaN structures ISWA after RIE process in function of a) aspect ratio and b) trenches width for different structures depth (280, 625 and 920 nm) and trenches width (from 2.9 to 19 µm) characterised using AFM

At the condition of constant structures depth, the influence of structures width on structures ISWA after RIE process can be represent by empirical equation form as follows:

$$(5) \qquad \alpha = A \cdot \exp(\frac{B}{w+C})$$

where w is structures width, and A, B, C are empirical tconstants. The empirical Eqs. (6 – 8) represent the influence of structures width on structures ISWA after RIE process, for each structures depth studied in this article as follow:

$$(6) \qquad \alpha_{d=280nm} = 20{,}92 \exp(\frac{4{,}91}{w+2{,}34})$$

$$(7) \qquad \alpha_{d=625nm} = 26{,}35 \exp(\frac{3{,}03}{w+1{,}08})$$

$$(8) \qquad \alpha_{d=920nm} = 21{,}82 \exp(\frac{4{,}19}{w-1{,}45})$$

The empirical constants A, B, C in Eq. (5) depend on structures depth, therefore the influence of structures depth on this constants was described by polynomial empirical equations. The empirical constants A, B, C in Eq. (5) were replaced by this polynomial equations, which resulted in the final form of empirical equation which describes the influence of structures width and depth on ISWA after RIE process as follows:

$$(9) \quad \alpha = (-48{,}57\,d^2 + 59{,}7\,d + 8{,}01)exp\frac{14{,}66\,d^2-18{,}71\,d+9}{w+7{,}69\,d^2-3{,}31\,d-2{,}02})$$

The structures ISWA measured using SEM were calculated as follows:

$$(10) \qquad tg\,\alpha = \frac{2\cdot d}{w_i^t - w_t^i}$$

Based on the Eq. (10) and the SEM results, the influence of the structures width on the structures ISWA was presented in Fig. 6: island ISWA (a) and trenches ISWA (b). The drop of structures ISWA in function of structures width was not monotonic. According to SEM results, the structures width has less impact on the structures ISWA than according to AFM results. The average structures ISWA was calculated for entire substrates with different width islands and trenches, on the basis of AFM and SEM measurements. The average structures ISWA after RIE process in function of the structures depth is presented in Fig. 7: AFM results (a) and SEM results (b). The selectivity of etching [semiconductor: mask] was dropping regular in function of process duration and structures depth. The mask ISWA of samples etched to the 280 nm depth, before RIE process was 18°, and the mask ISWA of samples etched to the 625, and 920 nm, before RIE process have 31°. According to Eq. (4), with increasing of mask ISWA should increase the GaN structures ISWA obtained after RIE process. The SEM results of 280 and 625 nm structures depth pointing to the opposite phenomenon than predicted by Eq. (4), and the AFM results. According to Eq. (4), decreasing selectivity should result in decreasing the structures ISWA after RIE process. The SEM results of samples with 625 and 920 nm structures depth, pointing to the opposite phenomenon than predicted by Eq. (4), and the AFM results. The structures slope is created during RIE process by completely etching the mask slope as is presented in Fig. 8. The etched mask slope width (Δb) depends on the mask ISWA, and the etching selectivity and duration. The width of the completely etched mask slope was respectively: 215, 324 and 575 nm.

The differences between AFM and SEM results are compared to the completely etched mask ISWA and slope width in Table 2.
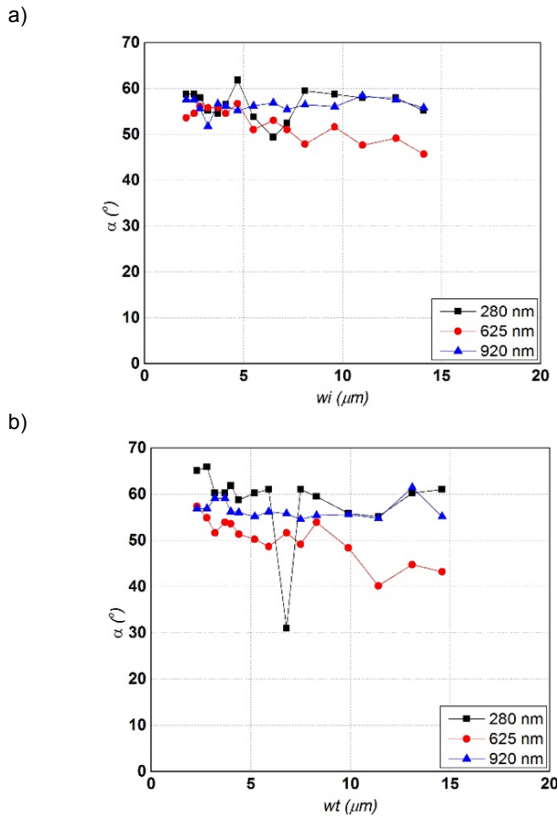
a)

b)

Fig. 6 The structures ISWA of a) islands and b) trenches in function of structures width, measured using SEM

Table 2. Differences between AFM and SEM results compared to the completely etched mask ISWA and slope width

sh [nm]	Φ [°]	Δb [nm]	α_SEM - α_AFM [°]	tg (α_SEM) - tg (α_AFM)
280	18	215	21	0,79
625	31	324	7	0,27
920	31	575	17	0,67

The increase of the slope width of completely etched mask of 77%, from 324 to 575 nm caused increase of the difference between SEM result tangent and AFM result tangent of 248%. The increase of the mask ISWA of 72%, from 18 to 31 degree, and etched mask slope width of 51%, from 215 to 324 nm, caused drop of the difference between SEM result tangent and AFM result tangent of 66%. Result presented in Tab. 2 lead to the conclusion that the increase of the completely etched mask slope width causes increase difference between SEM and AFM result. However, the increase of the mask ISWA causes drop of the difference between SEM and AFM result.
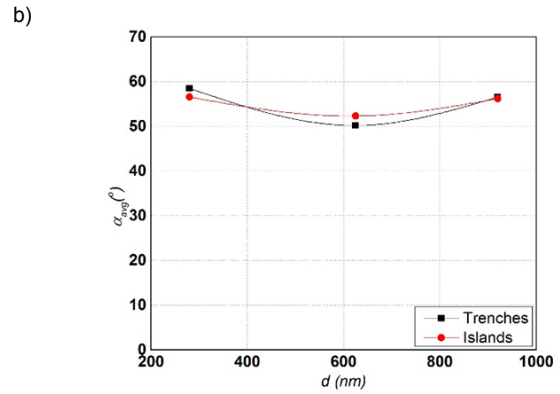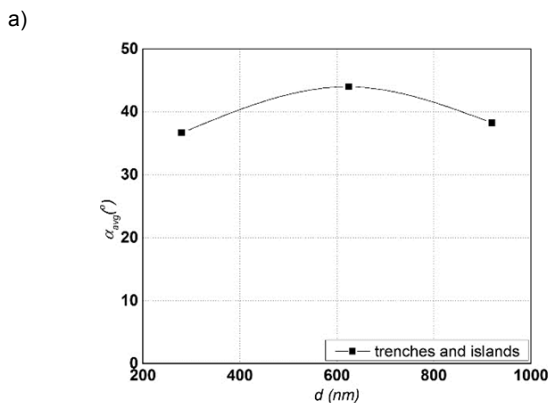
a)

b)

Fig. 7 Comparison of average structures ISWA after RIE process in function of structures depth, characterised using a) AFM and b) SEM
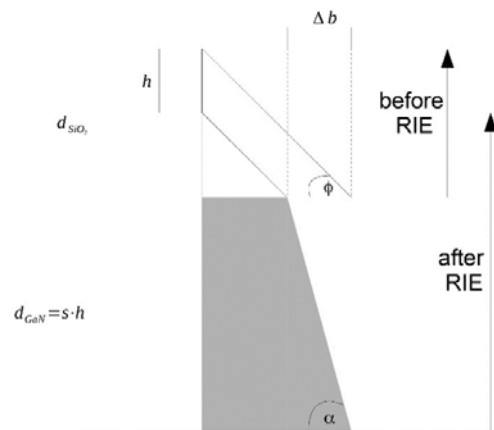

Fig. 8 The construction lines presenting the mask profile before RIE process and the mask-strutures profile after RIE process as the structures slope created by completely etched mask slope

Despite that plasma etching by nature is an anisotropy etching, the difference between the side walls inclination of the gained structures and theoretical inclination according to Eqs (3, 4) leads to the conclusion that on the structures profile have significant impact the conditions of the RIE process which define the anisotropy degree. Through the selection of mask materials and RIE conditions, the fabrication of piezotronic structures with given natural frequencies is possible. Ion etching of structures using mask allow to copy mask pattern to the structure with the proportions depending on the selectivity and anisotropy of RIE process. Magnitude of mask ISWA and structures ISWA in function of pattern width are not converging. Comparison of mask ISWA in Fig. 2: (b) with structures ISWA in Fig. 5: (a) and (b) leads to the conclusion that observed effect is independent on mask ISWA, however pattern width in mask have influence on the RIE anisotropy. In the Fig. 9, the evolution of structures depth in function of pattern width is presented. The increase of window width in etched mask can cause drop of etch rate or increase of etch rate. The drop of etch rate, caused by increase of window width in etched mask understood as increase of the etched surface area is associated with loading effect. However, the increase of etch rate, caused by increase of window width in etched mask is associated with a set of mechanisms called ARDE. The small changes of depth of the structures etched via mask windows of different width lead to the conclusions that the set of ARDE mechanisms and depleted concentration of ions above the wide windows of mask, caused quasi-uniform etch rate on the entire substrate in this study.
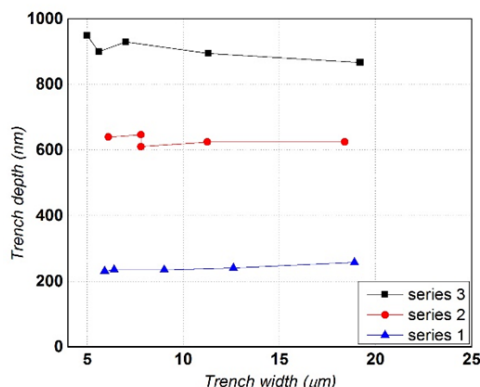
Fig. 9 The influence of window width on etch rate in mutual compensation of micro-loading and RIE-lag

In the literature, theoretical etch rate is defined by Eq. 11 [11] as follows:

$$(11) \qquad R = \frac{6{,}22 \; s_y \cdot j \cdot M}{\rho}$$

where s_y is the sputter yield, j the ion flux (mA/cm2), M the molecular weight of the etched material (g/mol), and ρ the density of the material to be etched (g/cm3).

If density and energy of ions that bombard silicon dioxide surface and gallium nitride surface, were similar, theoretical selectivity, calculated as ratio of etch rate equations 4 [GaN: SiO_2] would by 0,35. Empirical selectivity of etching at the beginning of RIE process was approximately 4. This result leads to the conclusion that the layer of silicon dioxide load with positive charges and deflects Ar^+ ions trajectories in direction to the mask window.

Summary

In this article the results of the study on RIE process of GaN structures using silicon dioxide layer as hard mask are presented. Obtained structures were measured for study on profiles evolution in function of structures width and depth. The empirical solution is presented to determine the approximate value of the structures ISWA which depends on structures width and depth. The increase of the structures width caused drop of the structures ISWA. This effect was caused by evolution of anisotropy degree on the entire substrate. The comparison of the SEM and AFM results leads to the conclusions that the structures side walls, created by etching via wide slope and low ISWA mask, are very difficult to characterisation. This effect should by more studied in the near time.

Acknowledgement

Authors:
mgr inż. Sławomir Owczarzak,
E-mail: Slawomir.Owczarzak@pwr.edu.pl,
dr inż. Andrzej Stafiniak,
E-mail: Andrzej.Stafiniak@pwr.edu.pl,
dr inż. Joanna Prażmowska,
Joanna.Prazmowska@pwr.edu.pl,
prof. dr hab. inż. Regina Paszkiewicz,
E-mail: Regina.Paszkiewicz@pwr.edu.pl,
Faculty of Microsystem Electronics and Phtonics, Wrocław University of Science and Technology, Janiszewskiego 11/17, 50-372 Wrocław, Poland

REFERENCES
[1] Karttunen J., Kiihamäki J., Franssila S., Loading effects in deep silicon etching, Proceedings of SPIE 2000. Vol. 4174, pp. 90–97. © International Society of Optical Engineering (SPIE)
[2] Jansen H., de Boer M., Burger J, Legtenberg R., and Elwenspoek M., THE BLACK SILICON METHOD H: THE EFFECT OF MASK MATERIAL AND LOADING ON THE REACTIVE ION ETCHING OF DEEP SILICON TRENCHES, Microelectronic Engineering 27 (1095) 475-480
[3] Hedlund C., Blom H. O., and Berg S., Microloading effect in reactive ion etching, Journal of Vacuum Science & Technology A: Vacuum, Surfaces, and Films 12, 1962 (1994)
[4] Kato S., Sato M., and Arita Y., Microloading effect prevention in Si02 contact-hole etching, Journal of Vacuum Science & Technology A: Vacuum, Surfaces, and Films 12, 1204 (1994)
[5] Kiihamaki J. and Franssila S., *Pattern shape effects and artefacts in deep silicon etching,* Journal of Vacuum Science & Technology A: Vacuum, Surfaces, and Films 17, 2280 (1999)
[6] Lee Y.H. and Zhou Z.H., Feature-Size Dependence of Etch Rate in Reactive Ion Etching, J. Electrochem. Soc., Vol. 138, No. 8, August 1991
[7] Xie R.J., Kava J.D., and Siegel M., Aspect ratio dependent etching on metal etch: Modeling and experiment, Journal of Vacuum Science & Technology A: Vacuum, Surfaces, and Films 14, 1067 (1996)
[8] Gottscho R.A., Jurgensen C.W., and Vitkavage D.J., Microscopic uniformity in plasma etching, Journal of Vacuum Science & Technology B: Microelectronics and Nanometer Structures Processing, Measurement, and Phenomena 10, 2133 (1992)
[9] Tezcan D.S., De Munck K, Pham N., Luhn O., Aarts A., De Moor P., Baert K., and Van Hoof C., Development of Vertical and Tapered Via Etch for
[10] Li X, Abe T. and Esashi M., DEEP REACTIVE ION ETCHING OF PYREX GLASS, 0-7803-5273-4/001$10.00 02000 IEEE
[11] Hays D.C., Selective etching of compound semiconductors, A thesis presented to the graduate school of The University of Florida in partial fulfillment of the requirements for the degree of master of science University of Florida 1999